Inhibition of Jun NH_2-Terminal Kinases Suppresses the Growth of Experimental Head and Neck Squamous Cell Carcinoma

Neil D. Gross,[1] Jay O. Boyle,[2] Baoheng Du,[4] Vikram D. Kekatpure,[2,4] Agnieszka Lantowski,[4] Howard T. Thaler,[3] Babette B. Weksler,[4] Kotha Subbaramaiah,[4] and Andrew J. Dannenberg[4]

Abstract

Purpose: This study was carried out to investigate whether c-Jun NH_2-terminal kinases (JNK) are potential targets for treating head and neck squamous cell carcinoma (HNSCC).

Experimental Design: JNK activity was first evaluated in 20 paired samples of human HNSCC. The antitumor activity of SP600125, a reversible nonselective ATP-competitive inhibitor of JNKs, was then investigated both in an HNSCC xenograft model and *in vitro* using immunohistochemistry, immunoblotting, enzyme immunoassay, flow cytometry, and a Matrigel assay of capillary tube formation. Complementary studies were carried out using small interfering RNA to JNK1/2.

Results: JNK activity was increased in human HNSCC compared with normal-appearing epithelium. Treatment of mice bearing HNSCC xenografts with SP600125 resulted in >60% inhibition of tumor growth relative to vehicle-treated animals. Inhibition of tumor growth was associated with significant reductions in both cell proliferation and microvessel density. SP600125 inhibited tumor cell proliferation by causing delays in both the S and G_2-M phases of the cell cycle. Inhibition of angiogenesis seemed to reflect effects on both tumor and endothelial cells. The JNK inhibitor suppressed the production of vascular endothelial growth factor and interleukin-8 by tumor cells and also inhibited endothelial cell proliferation and capillary tube formation. Reduced amounts and phosphorylation of epidermal growth factor receptor were found in tumor cells after treatment with SP600125. Small interfering RNA – mediated suppression of JNK1/2 led to reduced tumor cell proliferation and decreased levels of epidermal growth factor receptor, vascular endothelial growth factor, and interleukin-8.

Conclusions: JNK activity is commonly increased in HNSCC. Our preclinical results provide a rationale for evaluating JNK inhibition as an approach to treating HNSCC.

The c-Jun NH_2-terminal kinases (JNK) are members of the mitogen-activated protein kinase family that, when stimulated, regulate a variety of cellular activities, including proliferation, differentiation, and tumorigenesis (1, 2). There are three *JNK* genes. *JNK1* and *JNK2* gene expression is ubiquitous, whereas JNK3 expression is largely restricted to the heart, testis, and brain (3). The JNKs are activated in response to environmental stresses, inflammatory cytokines, and extracellular stimuli, including epidermal growth factor (4, 5). JNKs are serine/threonine protein kinases that phosphorylate a number of transcription factors, including the c-Jun component of the activator protein-1 (AP-1) transcription factor complex. AP-1 activation is important in cell transformation (6) and skin tumor formation in mice (7). In fact, JNK activation and c-Jun phosphorylation are required for transformation induced by *Ras*, an oncogene that is mutationally activated in ~30% of human malignancies (8) and frequently overexpressed in head and neck squamous cell carcinoma (HNSCC; ref. 9). Genetic and pharmacologic approaches have been used to evaluate the potential importance of JNKs in tumor formation and growth. Antisense oligonucleotides to JNKs suppressed the growth of tumor cells and inhibited the growth of PC3 prostate cancer xenografts (10). SP600125, a reversible, nonselective ATP-competitive inhibitor of JNK, suppressed the growth of both human prostate carcinoma xenografts and murine Lewis lung carcinoma (11). In another study, JNKs were found to be activated in a subset of human non – small cell lung cancers and to promote oncogenesis in the bronchial epithelium (12).

Although there is emerging preclinical evidence that inhibiting JNKs may be a useful approach to suppressing tumor growth, little is known about which tumor types to target. In the present study, we first determined that JNK activity was increased in human HNSCC compared with normal epithelium. Subsequently, we showed that SP600125 suppressed the growth of HNSCC xenografts by inhibiting tumor cell proliferation and angiogenesis. Complementary *in vitro* studies suggested that the JNK inhibitor acted on both tumor and endothelial cells to mediate tumor growth

Authors' Affiliations: [1]Department of Otolaryngology-Head and Neck Surgery, Oregon Health and Science University, Portland, Oregon; Departments of [2]Surgery (Head and Neck Service) and [3]Epidemiology and Biostatistics, Memorial Sloan-Kettering Cancer Center; and [4]Department of Medicine, Weill Medical College of Cornell University, New York, New York

Received 2/12/07; revised 6/27/07; accepted 7/3/07.

Grant support: NIH grants T32 CA09685 and RO1HL55627, and the Center for Cancer Prevention Research.

The costs of publication of this article were defrayed in part by the payment of page charges. This article must therefore be hereby marked *advertisement* in accordance with 18 U.S.C. Section 1734 solely to indicate this fact.

Requests for reprints: Andrew J. Dannenberg, New York Presbyterian-Cornell, 525 East 68th Street, Room F-206, New York, NY 10021. Phone: 212-746-4403; Fax: 212-746-4885; E-mail: ajdannen@med.cornell.edu.

doi:10.1158/1078-0432.CCR-07-0352

inhibition. Taken together, these data highlight the potential importance of targeting JNKs as a therapeutic strategy for treating HNSCC.

Materials and Methods

Materials. DMEM/F12 and fetal bovine serum were from Invitrogen. Keratinocyte growth medium, EBM-2, and SingleQuots kits were from Clonetics Corp. Eagle's MEM was from American Type Culture Collection, and RPMI 1640 was from Life Technologies. SP600125 was a gift from the Signal Research Division of Celegene Corp. Matrigel was from BD Biosciences and male immunodeficient *nu/nu* mice were from Charles River Laboratories. The stress-activated protein kinase/JNK assay kit was from Cell Signaling Technology. Antibodies to human phosphorylated c-Jun, JNK, total epidermal growth factor receptor (EGFR), and the phosphorylated c-Jun standard were from Santa Cruz Biotechnology. Anti–phosphorylated EGFR antiserum was from Upstate. Anti-mouse CD34 antiserum was from PharMingen. Anti–Ki-67 (MIB-1) was obtained from Immunotech. Vector stain was from Vector Laboratories. 3-(4,5-Dimethylthiazol-2-yl)-2,5-diphenyltetrazolium bromide (MTT), carboxymethylcellulose, Tween 80, RNase A, lactate dehydrogenase diagnostic kits, anti–β-actin antibody, and Lowry protein assay kits were from Sigma Chemical. Nitrocellulose membranes were from Schleicher & Schuell. Enhanced chemiluminescence Western blotting detection reagents were from Perkin-Elmer Life Sciences, Inc. RNA was prepared using kits from Qiagen. Quantikine human vascular endothelial growth factor (VEGF) and human CXCL8/interleukin-8 (IL-8) immunoassay kits were from R&D Systems.

Human specimens. Twenty paired samples (tumor and adjacent normal-appearing mucosa) were collected during surgical resection of HNSCC at Memorial Sloan-Kettering Cancer Center. Normal oral mucosa was also obtained from 10 cancer-free subjects. The specimens (~2 × 2 mm) were sharply excised, placed in sterile cryovials, snap-frozen in liquid nitrogen, and maintained at -80°C. This study was approved by the Committees on Human Rights Research at Memorial Sloan-Kettering Cancer Center and Weill Cornell Medical College.

HNSCC xenografts. HNSCC xenografts were established by implanting 1483 cells (2.5×10^5) suspended in 30% Matrigel s.c. into the flanks of 7-week-old male *nu/nu* mice. Once the tumors became palpable, 20 mice were assigned to daily treatment via i.p. injection (0.5 mL) with either SP600125 (50 mg/kg) or vehicle (0.5% carboxymethylcellulose and 0.25% Tween 80). Tumor growth was assessed twice each week by caliper measurement of tumor diameter in the longest dimension (L) and at right angles to that axis (W). Tumor volume was estimated using the formula $L \times W \times W \times \pi/6$. The Institutional Animal Care and Use Committee at Weill Cornell Medical College approved the protocol.

Cell culture. 1483 HNSCC cells (13) were cultured in DMEM/F12 supplemented with 10% fetal bovine serum, 100 IU/mL penicillin G, and 100 μg/mL streptomycin. The MSK-Leuk1 cell line was established from a dysplastic leukoplakia lesion adjacent to a squamous cell carcinoma of the tongue (14). This cell line was routinely maintained in keratinocyte growth medium supplemented with bovine pituitary extract. The Ca9-22 cell line was derived from human gingival HNSCC and grown in Eagle's MEM supplemented with 10% fetal bovine serum (15). The 012 HNSCC cell line was maintained in RPMI 1640 supplemented with 10% fetal bovine serum (16). The 886Ln cell line was established from a lymph node metastasis of a poorly to moderately differentiated laryngeal HNSCC (17). D3 immortalized human endothelial cells (18) were cultured in CT2X (EBM-2 supplemented with growth factors, 5% fetal bovine serum, and 100 μg/mL gentamicin) diluted 1:4 with EGM-2 medium. Cells were grown at 37°C in a humidified 5% CO_2 incubator. All treatments with SP600125 or vehicle (0.1% DMSO) were carried out in the presence of serum or growth medium (MSK-Leuk1). Cellular cytotoxicity was assessed by measurements of cell counts and lactate dehydrogenase release. There was no evidence of cytotoxicity in any of the experiments.

JNK activity. JNK activity was assessed in human and xenograft tissues using a stress-activated protein kinase/JNK assay kit. Lysates were prepared by probe sonicating tissue specimens in lysis buffer for 3 × 10 s on ice and centrifuging at 10,000 × *g* for 10 min to sediment particulate material. The protein concentration of the supernatant was measured by the method of Lowry et al. (19). Tissue lysate protein (100 μg) was diluted with lysis buffer to a volume of 250 μL and incubated overnight with 20 μL c-Jun fusion beads at 4°C. Lysates were then recentrifuged and washed with lysis buffer (×2) and kinase buffer (×2) to eliminate nonspecific binding. Lysates were suspended in kinase buffer supplemented with 100 μmol/L ATP and incubated for 30 min at 30°C. The reaction was terminated and c-Jun phosphorylation was assessed via Western blot analysis.

Immunohistochemistry. Proliferation and angiogenesis were evaluated by staining for Ki-67 and CD34 as described previously (20–22). Neutral buffered formalin-fixed tissue was embedded in paraffin. Tissue sections (5 μm) were prepared using a microtome and mounted on slides. Sections were deparaffinized in xylene, rehydrated in graded alcohols, and washed in distilled water. Endogenous peroxidase was quenched with 0.01% H_2O_2. Antigen retrieval was done by microwaving the sections in 10 mmol/L citric acid (pH 6.0) for 30 min. In addition, sections for Ki-67 analysis were treated with 0.05% trypsin, 0.05% $CaCl_2$ in Tris-HCl (pH 7.6) for 5 min at 37°C before microwave treatment. The slides were washed thrice in PBS and blocked for 30 min with 10% normal rabbit serum (CD34) or 10% normal horse serum (Ki-67). Tissue sections were then incubated with antiserum to mouse CD34 at 25 μg/mL and antiserum to Ki-67 at a 1:5,000 dilution (2% bovine serum albumin in PBS) and incubated overnight at 4°C. After being washed thrice with PBS, the sections were incubated with biotinylated anti-mouse immunoglobulins at 1:100 (CD34) or 1:500 (Ki-67) dilution for 30 min at room temperature. The slides were then washed thrice in PBS and labeled using 1:25 avidin-biotin peroxidase complexes (Vector Stain) for 30 min at room temperature. The reaction was visualized using 3,3-diaminobenzidine. Subsequently, the slides were rinsed in tap water and counterstained with hematoxylin. The slides were then dehydrated with ethanol, rinsed with xylene, and mounted.

Proliferation was assessed by counting the number of tumor cells with Ki-67–positive nuclei and the total number of tumor cells at ×400 magnification in three representative regions of the tumor. Results are expressed as the proliferation index: proportion of positively staining cells over the total number of cells. Microvessel density was assessed by counting the number of microvessels at ×400 magnification in three fields that had the highest vascularization. The results are expressed as an average number of microvessels per field.

Western blotting. Lysates were prepared by treating cells with lysis buffer [100 mmol/L Tris-HCl (pH 7.5), 50 mmol/L NaCl, 50 mmol/L NaF, 30 mmol/L sodium PPi, 1 mmol/L EDTA, 1% Tween 20, 1 mmol/L Na_3VO_4, 5 μg/mL aprotinin, complete mini protease inhibitor mixture, and 5 μmol/L 3,4-dichlorocoumarin]. Lysates were sonicated for 5 min on ice and centrifuged at 10,000 × *g* for 10 min to sediment the particulate material. The protein concentration of the supernatant was

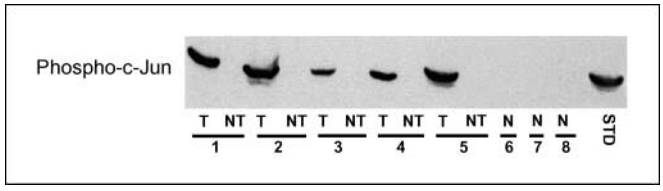

Fig. 1. JNK activity is increased in HNSCC. JNK activity was measured by immunoprecipitation of JNK coupled with a kinase assay using c-Jun as substrate. JNK activity was consistently elevated in HNSCC (*T*) compared with adjacent normal-appearing epithelium (*NT*; subjects 1-5) or normal oral epithelium (*N*) from healthy volunteers (subjects 6-8).

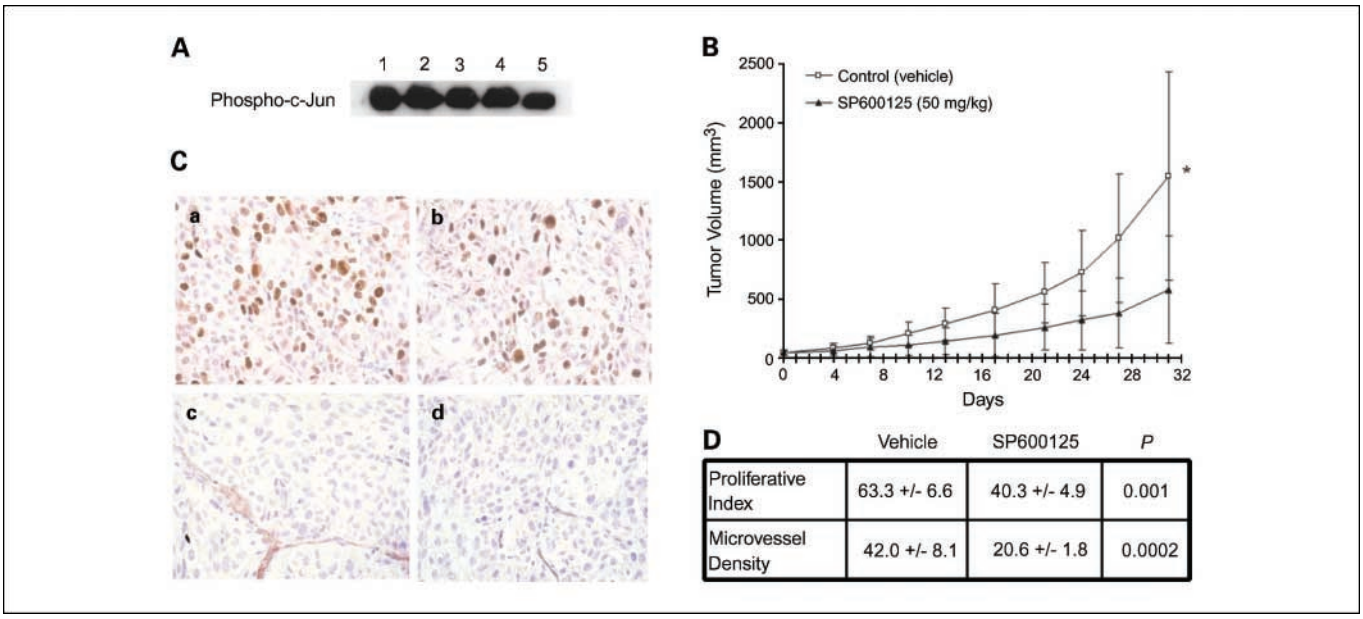

Fig. 2. SP600125 inhibits HNSCC xenograft growth. *A,* JNK activity is shown in 1483 cell HNSCC xenografts ($n = 5$). *B,* daily treatment with SP600125 resulted in significant inhibition of the growth of 1483 xenografts relative to treatment with vehicle. 1483 cells were inoculated into the flanks of nude mice. Once tumors became palpable, mice were treated daily with vehicle ($n = 9$) or SP600125 ($n = 11$). Tumor volume was assessed at multiple time points. Points, mean; bars, SD. $^*P < 0.001$. *C,* after treatment for ~1 mo, tumor tissue was obtained, formalin-fixed, and paraffin-embedded. Immunohistochemistry was done to assess cell proliferation (Ki-67) and vascular density (CD34). Representative tumor sections stained for Ki-67 are shown (×400) from mice treated with vehicle (*a*) or SP600125 (*b*). Representative tumor sections stained for CD34 are shown (×400) from mice treated with vehicle (*c*) or SP600125 (*d*). *D,* summary of the findings for proliferation index and microvessel density in tumors from mice treated with vehicle or SP600125. Data are presented as means ± SD; $n = 6$/group.

measured by the method of Lowry et al. (19). SDS-PAGE was done under reducing conditions on 7.5% or 10% polyacrylamide gels as described by Laemmli (23). The resolved proteins were transferred onto nitrocellulose sheets as detailed by Towbin et al. (24). The nitrocellulose membrane was then incubated with primary antibodies. Secondary antibody to IgG conjugated to horseradish peroxidase was used. The blots were probed with enhanced chemiluminescence Western blot detection system according to the manufacturer's instructions.

Cell growth analysis. Cells were plated (2×10^3 per well) in 96-well plates and were allowed to adhere overnight before being treated with vehicle or SP600125. Fresh medium containing vehicle or the indicated concentration of SP600125 was added every 2 days. At each time point, the culture medium was removed and replaced with MTT (0.5 mg/mL). The reaction was stopped 3 h later by removing the medium and immediately solubilized by adding 100 μL DMSO. Absorbance was measured after 10 min at 560 nm in a 96-well plate reader.

DNA synthesis. Incorporation of [^{3}H]thymidine was used to measure DNA synthesis. 1483 and D3 cells plated (2×10^3 per well) in 96-well plates were allowed to adhere overnight before being treated with vehicle or SP600125. After 18 h of treatment at 37°C, the medium was supplemented with [^{3}H]thymidine (0.1 μCi/well) for 6 h. Cells were then washed thrice with PBS. Radioactivity was measured with a LS6800 liquid scintillation counter from Beckman.

Cell cycle analysis. 1483 cells were treated with vehicle (0.1% DMSO) or 25 μmol/L SP600125 for 24 h. The cells were released by treatment with trypsin-EDTA, washed, and suspended in ice-cold PBS (pH 7.4), counted, and fixed overnight in 50% ethanol at 4°C. The cells (10^6/mL) were then resuspended in 1.12% sodium citrate with RNase A (500 units/mL) for 30 min at 37°C. Propidium iodide (50 μg/mL) was added and the cells were maintained in the dark for 30 min at room temperature. The red fluorescence of single events was recorded using an argon ion laser at 488-nm excitation wavelength and 610-nm emission wavelength to measure DNA index on a Coulter Epics XL flow cytometer. The percentage of cells present in each phase of the cell cycle was determined using ModFitLT V2.0 software from Verity Software House.

VEGF production. Amount of VEGF produced was quantified with Quantikine human VEGF immunoassay kit according to the manufacturer's instructions.

Measurements of IL-8. Total RNA was isolated using the RNeasy Mini Kit according to manufacturer's instructions. Reverse transcription was done using 2 μg of RNA per 50 μL of reaction. The reaction mixture contained 1× PCR Buffer II, 2.5 mmol/L $MgCl_2$, 0.5 mmol/L deoxynucleotide triphosphates, 2.5 μmol/L oligo(dT)16 primer, 50 units RNase inhibitor, and 125 units murine leukemia virus reverse transcriptase (Roche Applied Science). Samples were amplified in a thermocycler for 10 min at 25°C, 15 min at 42°C, 5 min at 99°C, and 5 min at 5°C. The resulting cDNA was used for amplification. The volume of the PCR reaction was 25 μL and contained 5 μL of cDNA, 1× PCR Buffer II, 2 mmol/L $MgCl_2$, 0.4 mmol/L deoxynucleotide triphosphates, 400 nmol/L forward primer, 400 nmol/L reverse primer, and 2.5 units Taq polymerase (Applied Biosystems). Samples were denatured at 95°C for 2 min and then amplified for 35 cycles in a thermocycler under the following conditions: 95°C for 30 s, 62°C for 30 s, and 72°C for 45 s. Subsequently, the extension was carried out at 72°C for 10 min. Primer sequences were as follows: IL-8, sense 5′-AGGGTTGCCAGATGCAATAC-3′, antisense 5′-AAACCAAGGCACAGTGGAAC-3′; β-actin, sense 5′-GGTCACCCACACTGTGCCCAT-3′, antisense 5′-GGATGCCACAGGACTCCATGC-3′. PCR products were subjected to electrophoresis on a 1% agarose gel with 0.5 μg/mL ethidium bromide. The identity of each PCR product was confirmed by DNA sequencing.

Amount of IL-8 protein produced was determined with a Quantikine human IL-8 immunoassay kit according to the manufacturer's instructions.

RNA interference. JNK1/JNK2 targeting small interfering RNA (siRNA) was custom synthesized by Dharmacon. Sequences were as follows: sense 5′-TGAAAGAATGTCCTACCTT-3′ and antisense 5′-AAGGTAGGACATTCTTTCA-3′ (25). Nonspecific control siRNA was also obtained from Dharmacon. Cells were seeded in DMEM and 10% fetal bovine serum for 24 h before transfection. siRNA to JNK1/2 or nonspecific siRNA (both 100 pmol/mL) was transfected using

DharmaFECT 4 transfection reagent according to the manufacturer's instructions.

Angiogenesis. Matrigel (150 μL/well) was added to 48-well plates and incubated at 37°C for at least 30 min before use. D3 cells grown to confluency were detached by treatment with trypsin-EDTA, counted, and resuspended in 1:4 diluted CT2X to a concentration of 1×10^5 cells/mL. The cells were then mixed with 0 to 20 μmol/L SP600125, plated onto the Matrigel surface of the 48-well plates, and incubated at 37°C for 18 h. Capillary tube formation was assessed. Representative images were captured digitally for each condition at ×40.

Statistics. Xenograft tumor growth was compared using repeated measures ANOVA to the cubed-root of volumes. Statistical significance of difference in growth rate between SP600125 and control was based on comparison of linear trends in the transformed scale. Results are expressed descriptively as the mean ± SE. All other comparisons between groups were made by the two-tailed Student's *t* test with results presented as the mean ± SD using Microsoft Excel 2000 (Microsoft Corp.). A difference between groups of $P < 0.05$ was considered significant.

Results

JNK activity is increased in HNSCC. JNK activity was evaluated by Western blot in 20-paired HNSCC specimens (tumor versus adjacent normal appearing mucosa). Activity was also determined in oral mucosal biopsies from 10 healthy volunteers. A representative Western blot is shown in Fig. 1. JNK activity was elevated in HNSCC compared with normal mucosa. More specifically, JNK activity was easily detected in 95% of tumor samples but only 10% of adjacent normal-appearing mucosal samples. JNK activity was not detected in control specimens from healthy volunteers.

Inhibiting JNK suppresses the growth of HNSCC xenografts. To explore the role of JNKs as potential therapeutic targets, 1483 cell HNSCC xenografts were established and confirmed to have JNK activity similar to human tumors (Fig. 2A). Subsequently, nude mice xenografted with 1483 cells were randomized to treatment with either vehicle or SP600125, a JNK inhibitor. Daily treatment with SP600125 (50 mg/kg) for ~1 month resulted in >60% reduction in tumor volume ($P < 0.001$; Fig. 2B). Subsequently, measurements of cell proliferation and angiogenesis were carried out to explore the potential mechanisms underlying the antitumor activity of the JNK inhibitor. Nuclear staining of Ki-67 was used to assess cell proliferation. Treatment with SP600125 led to an ~36% decrease in cell proliferation ($P = 0.001$; Fig. 2Ca, Cb, and D). Angiogenesis was evaluated by staining for CD34, an antigen present in endothelial cells. Microvessel density decreased by >50% in tumors from mice treated with SP600125 ($P < 0.001$; Fig. 2Cc, Cd, and D). Taken together, these findings suggest that JNK activity is an important determinant of both tumor cell proliferation and angiogenesis in HNSCC.

Inhibition of JNKs suppresses tumor cell proliferation and angiogenesis. Experiments were next carried out to further

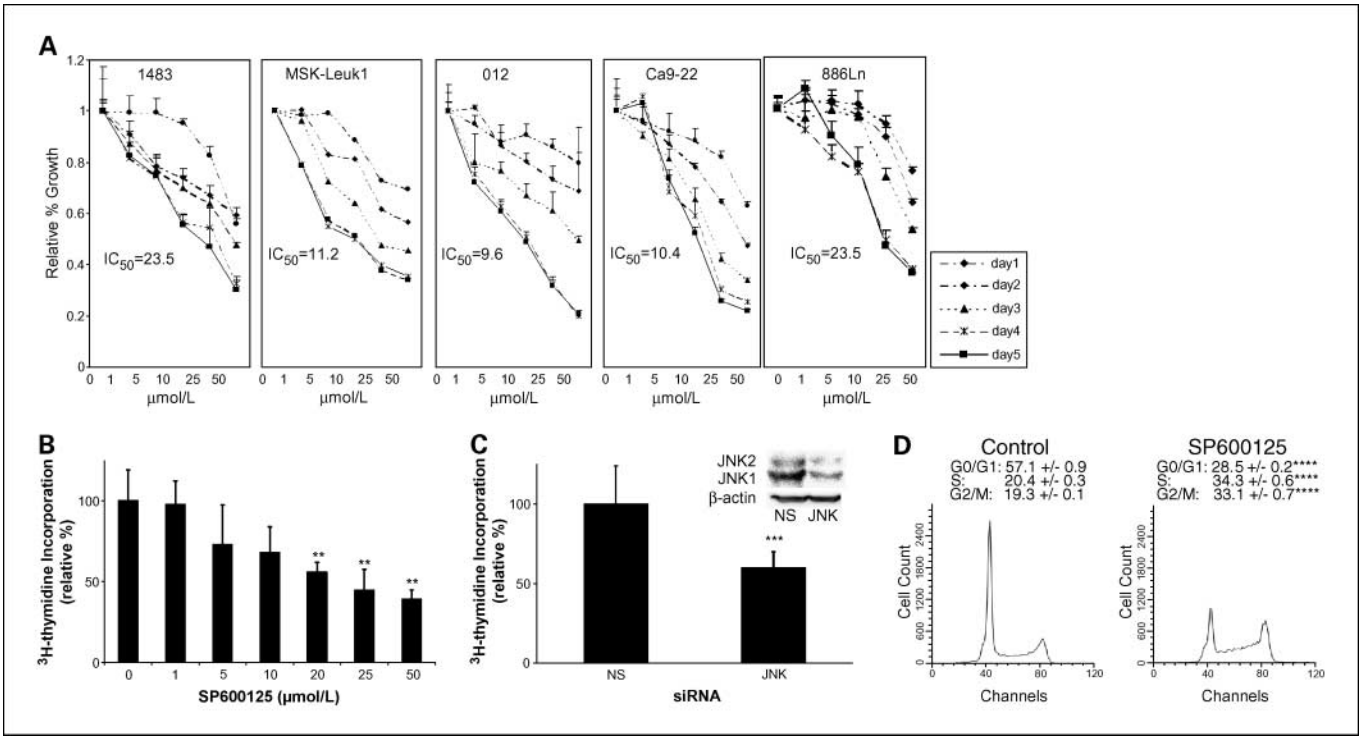

Fig. 3. SP600125 inhibited the proliferation of HNSCC cell lines. *A,* cell lines derived from leukoplakia (*MSK-Leuk1*), HNSCC (*1483, 012, CA9-22*), and metastatic HNSCC (*886Ln*) were treated with 0 to 50 μmol/L SP600125 for 1 to 5 d. Cell number was assessed by MTT assay and expressed relative to vehicle-treated cell number. The IC_{50} for SP600125 on day 5 is indicated. Points, mean ($n = 6$); bars, SD. *B,* 1483 cells were treated with 0 to 50 μmol/L SP600125. After 18 h of treatment, [^{3}H]thymidine was added for 6 h and DNA synthesis was quantified. [^{3}H]thymidine incorporation was expressed relative to vehicle-treated cells. Columns, mean ($n = 6$); bars, SD. *C,* immunoblot analysis shows that siRNA to JNK1/2 led to a marked reduction in both JNK1 and JNK2 protein in 1483 cells. 1483 cells were transfected with nonspecific (*NS*) siRNA or siRNA to JNK1 and JNK2 for 36 h. Subsequently, [^{3}H]thymidine was added for 6 h and DNA synthesis was quantified. Columns, mean ($n = 6$); bars, SD. *D,* representative DNA histogram of 1483 cells after treatment with vehicle (0.1% DMSO) or 25 μmol/L SP600125 for 18 h. SP600125 treatment resulted in an increased percentage of cells in the S and G_2-M phases relative to control. Indicated percentages represent a mean (±SD) of three independent experiments. $^{**}P < 0.01$, $^{***}P < 0.005$, and $^{****}P < 0.001$.

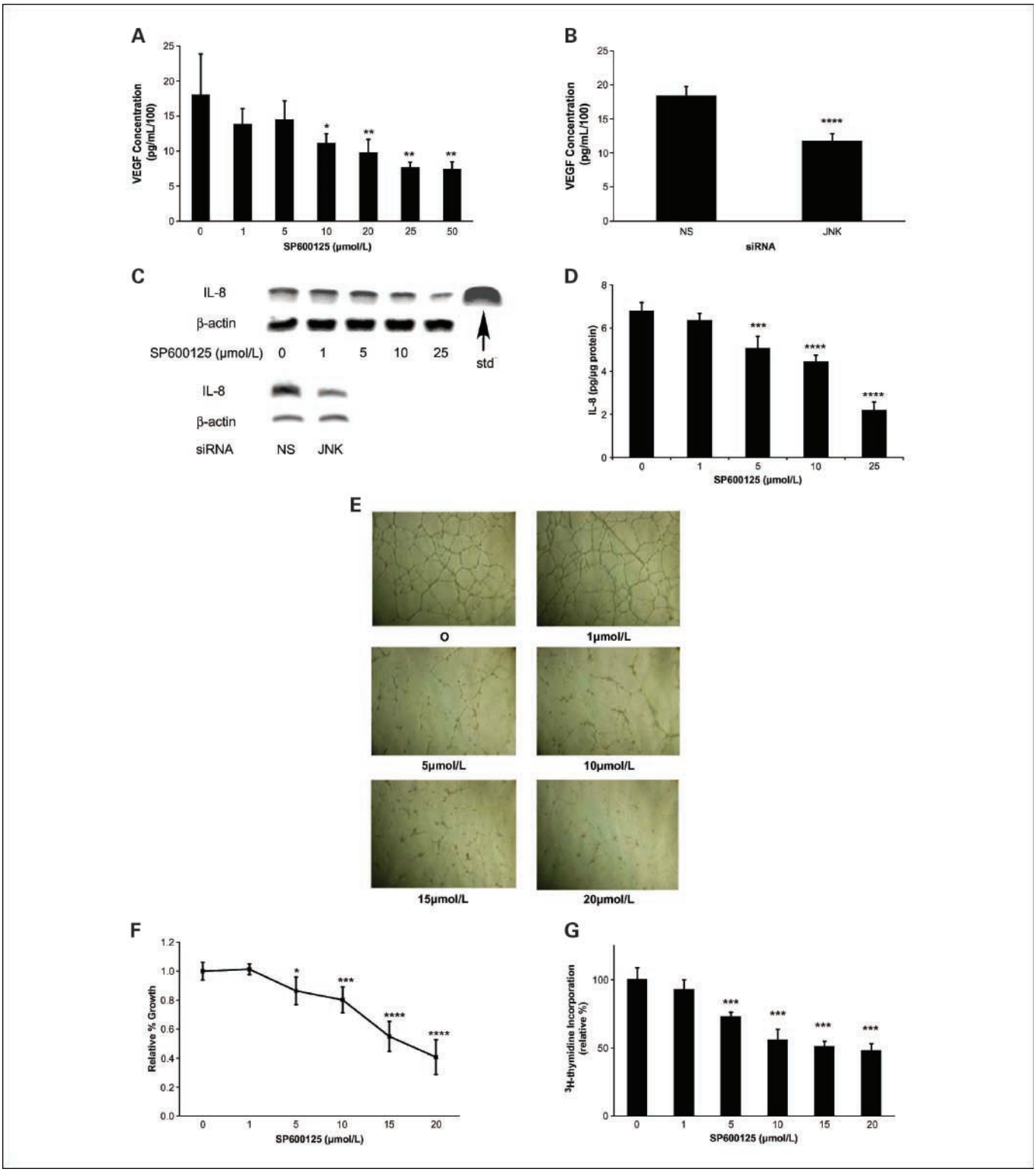

Fig. 4. JNK plays a role in tumor cell production of VEGF and IL-8 and endothelial capillary tube formation. *A,* 1483 cells were treated with 0 to 50 μmol/L SP600125 for 18 h before measuring VEGF protein production. *B,* VEGF production by 1483 cells is reduced after treatment with siRNA to JNK1 and JNK2. Following transfection with either nonspecific siRNA or siRNA to JNK1 and JNK2, VEGF production was measured. *C,* 1483 cells were treated with 0 to 25 μmol/L SP600125 for 24 h (*top*) or transfected with nonspecific siRNA or siRNA to JNK1 and JNK2 for 36 h (*bottom*). Subsequently, amounts of IL-8 and β-actin mRNA were determined by reverse transcription-PCR. *D,* 1483 cells were treated with 0 to 25 μmol/L SP600125 for 24 h before measuring the amount of IL-8 protein released into the medium. *E,* D3 endothelial cells were treated with 0 to 20 μmol/L SP600125 and plated onto Matrigel. Capillary tube formation was assessed qualitatively after 18 h of treatment. Representative images are presented at ×40 magnification. *F,* effect of SP600125 on endothelial cell proliferation. Cells were treated with the indicated concentration of SP600125 for 5 d. Cell number was assessed by MTT assay and expressed relative to vehicle-treated cell number. *G,* effect of SP600125 on DNA synthesis in endothelial cells. Cells were treated with 0 to 20 μmol/L SP600125. DNA synthesis was quantified after 18 h of treatment. [^{3}H]thymidine incorporation was expressed relative to vehicle-treated cells. Columns (*A, B, D*, and *G*), mean; bars, SD; $n = 6$; $^*P < 0.05$, $^{**}P < 0.01$, $^{***}P < 0.005$, and $^{****}P < 0.001$.

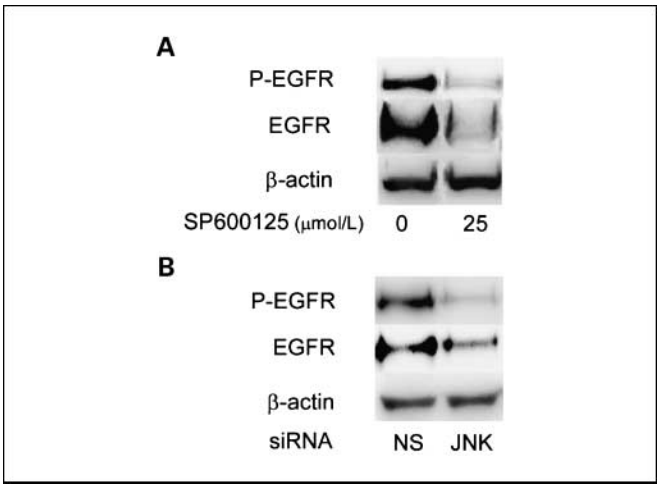

Fig. 5. Inhibiting JNKs suppressed the expression and phosphorylation of EGFR. 1483 cells were treated with vehicle or 25 μmol/L SP600125 for 24 h (*A*). Cells were also transfected with nonspecific siRNA or siRNA to JNK1 and JNK2 for 36 h (*B*). Cellular lysate protein (100 μg/lane) was then prepared and loaded onto a 7.5% SDS-polyacrylamide gel, electrophoresed, and subsequently transferred onto nitrocellulose. Immunoblots were probed as indicated.

evaluate the role of JNKs in regulating the growth of tumor cells. Consistent with our *in vivo* findings, *in vitro* treatment of 1483 HNSCC cells with SP600125 resulted in dose- and time-dependent growth inhibition (Fig. 3A) and diminished DNA synthesis (Fig. 3B). Cell number increased above the initial plating density during treatment, suggesting a cytostatic rather than a cytotoxic drug effect. To inhibit JNKs using an independent nonpharmacologic approach, we used siRNA directed against a common sequence of JNK1 and JNK2 (25). Figure 3C shows that transient transfection with this siRNA led to efficient down-regulation of both JNK1 and JNK2. Similar to the inhibitory effects of SP600125 (Fig. 3B), siRNA-mediated down-regulation of JNK1 and JNK2 led to a significant reduction in DNA synthesis (Fig. 3C). Next, we evaluated the effects of JNK inhibition on cell cycle progression. Treatment of 1483 cells with SP600125 led to a relative decrease in the percentage of cells in the G_0-G_1 phase and a corresponding increase in the percentage of cells in the S and G_2-M phases of the cell cycle (Fig. 3D), whereas no change in hypodiploidy occurred. To confirm that the growth-inhibitory effects of the JNK inhibitor were not unique to the 1483 HNSCC model, the effect of SP600125 on cell growth was evaluated in four other cell systems. Dose- and time-dependent growth inhibition was observed in cell lines derived from aneuploid leukoplakia (MSK-Leuk1), HNSCC (012, Ca9-22), and a lymph node metastasis derived from HNSCC (886Ln; Fig. 3A). The IC_{50} values for the five cell lines ranged from 9.6 to 23.5 μmol/L.

Because JNK inhibition resulted in decreased microvessel density in 1483 cell HNSCC xenografts (Fig. 2), complementary *in vitro* studies were carried out to evaluate the role of JNKs in angiogenesis. In theory, the antiangiogenic activity of SP600125 could have reflected effects on tumor cells, endothelial cells, or both. Hence, additional experiments were carried out in both tumor and endothelial cells. Treatment of 1483 cells with SP600125 resulted in a dose-dependent decrease in the production of VEGF, a proangiogenic factor linked to tumor growth (Fig. 4A). siRNA-mediated down-regulation of JNK1/2 also inhibited VEGF production (Fig. 4B). Because IL-8 is overexpressed in HNSCC (26) and implicated in angiogenesis (27, 28), we also evaluated the effects of JNK inhibition on IL-8 expression. Treatment with SP600125 suppressed the expression of IL-8 mRNA, a finding that was mimicked with siRNA-mediated suppression of JNK1 and JNK2 (Fig. 4C). The production of IL-8 protein was also suppressed by SP600125 (Fig. 4D). As mentioned above, the antiangiogenic effect of SP600125 observed in the HNSCC xenograft model could also have reflected direct effects on the endothelium. To investigate this possibility, the effect of JNK inhibition on endothelial cells was assessed. Using a Matrigel assay, we showed that the JNK inhibitor caused dose-dependent inhibition of endothelial capillary tube formation (Fig. 4E). Diminished capillary tube formation can be a consequence of multiple effects including reduced endothelial cell proliferation. Consistent with this idea, treatment with SP600125 resulted in dose-dependent inhibition of growth (Fig. 4F) and DNA synthesis (Fig. 4G).

Activation of JNKs stimulates AP-1–dependent induction of *EGFR* gene expression (29, 30). Inhibition of EGFR signaling is a recognized strategy for inhibiting tumor growth including HNSCC (31). Hence, to better understand the antitumor activity of SP600125, we also investigated whether inhibition of JNKs would suppress the expression and phosphorylation of EGFR in HNSCC tumor cells. Indeed, treatment with SP600125 led to reduced amounts of EGFR and phosphorylated EGFR (Fig. 5A). Importantly, these suppressive effects of SP600125 were mimicked by siRNA-mediated down-regulation of JNK1 and JNK2 (Fig. 5B).

Discussion

Targeted molecular therapies hold great promise for cancer treatment. In the case of aerodigestive malignancies, therapies that target the EGFR were recently found to improve the survival of patients with advanced-stage HNSCC (32) and non–small cell lung cancer (33). The fact that the survival benefits were modest underscores the need for additional therapies.

In the current study, we focused on the potential significance of JNKs as therapeutic targets for the treatment of HNSCC. The choice to investigate JNKs was based on prior evidence that JNKs and the AP-1 transcription factor complex are important for cell transformation, growth, differentiation, and angiogenesis (1, 34–36). We detected a marked increase in JNK activity in HNSCC compared with normal mucosa. Previously, activated extracellular signal-regulated kinases (ERK1/2), another mitogen-activated protein kinase subfamily, were found in HNSCC (37). Several potential mechanisms can explain the increased JNK activity in HNSCC. JNKs are activated by receptor tyrosine kinases including the EGFR (4). For example, activation of EGFR signaling stimulates the Ras-Raf-mitogen-activated protein kinase pathway. Because EGFR signaling is commonly activated in HNSCC (38), this is likely to contribute to the observed increase in JNK activity. In addition to receptor tyrosine kinases, cellular stress and cytokines activate JNKs (4). Interestingly, tobacco smoke can activate JNKs, at least in part, by oxidative stress (39). Each of these factors may contribute to the increase in JNK activity found in HNSCC.

To evaluate the potential significance of increased JNK activity in HNSCC, we used an HNSCC xenograft model.

Treatment with SP600125 caused a significant reduction in tumor growth. To investigate the mechanism underlying the growth-inhibitory effects of SP600125, measurements of cell proliferation and microvessel density were done. Treatment with SP600125 caused a significant reduction in both tumor cell proliferation and microvessel density. Subsequently, *in vitro* studies were carried out to further evaluate the importance of JNK activity in regulating tumor cell growth and angiogenesis. Tumor cell proliferation and [^{3}H]thymidine incorporation were suppressed by SP600125. In fact, the JNK inhibitor suppressed the growth of several cell lines, including those derived from leukoplakia, HNSCC, and a lymph node metastasis. Because small-molecule inhibitors can have off-target effects, siRNA to JNK1/2 was also used. Consistent with the findings for SP600125, down-regulation of JNK1 and JNK2 led to a significant reduction in DNA synthesis. The JNK inhibitor also caused an increase in the percentage of cells in the S and G_2-M phases of the cell cycle. JNK activity, which is increased in late S and G_2, has been shown to play a key role in cell cycle progression (34). Notably, treatment with SP600125 results in a reproducible slowing of cell cycle progression through the S and G_2 phases and induction of G_2-M arrest in multiple other models (11, 25).

The observed decrease in microvessel density in xenografts from mice treated with SP600125 could reflect effects on either tumor or endothelial cells. Notably, the AP-1 transcription factor complex can stimulate *VEGF* gene expression, a proangiogenic factor that is a recognized therapeutic target (40). We showed that treatment with either SP600125 or siRNA to JNK1/2 led to a significant reduction in VEGF production by 1483 cells. This finding is consistent with previous evidence that JNKs can regulate VEGF production in human gingival fibroblasts (41). Because VEGF can also stimulate JNK activity (35), it is possible that a JNK inhibitor could disrupt a positive feedback loop important for tumor growth. In addition to suppressing the production of VEGF, inhibition of JNKs led to reduced production of IL-8, a chemokine implicated in both HNSCC and angiogenesis (26–28). This finding is consistent with previous evidence that JNK activity can regulate IL-8 expression (42). Additionally, the JNK inhibitor had direct effects on endothelial cells. More specifically, endothelial cell proliferation and capillary tube formation were inhibited by treatment with the JNK inhibitor. Activation of EGFR signaling can activate JNKs and stimulate tumor cell proliferation and angiogenesis (4). Conversely, increased JNK signaling can induce the expression of EGFR, suggesting the existence of a positive feedback loop (29, 30). We showed that inhibition of JNKs led to reduced expression and phosphorylation of EGFR. The strong interdependence of these two molecules lends further support to the notion of targeting JNK activity as a strategy to inhibit tumor growth.

JNK activity is important for cell proliferation and cell cycle progression (34). As mentioned above, we found that JNK inhibition resulted in an increased percentage of cells in the S and G_2-M phases of the cell cycle. Tumor cells in G_2-M are highly sensitive to radiation (43). In fact, pharmacologic inhibition of JNKs has been reported to inhibit the repair of radiation-induced DNA damage and to increase radiation sensitivity (44). Both cisplatin and radiation, which are commonly used in combination for treatment of HNSCC, may be efficacious in cell killing in the S phase (45, 46). JNKs can be activated by radiation (47) and DNA-damaging agents such as cisplatin (48). Furthermore, activation of JNKs has been linked to DNA repair, raising the possibility that inhibition of JNKs could augment the activity of therapies that induce DNA damage (49). Based on the current findings, it would be logical to determine whether inhibition of JNKs before concurrent chemoradiation increased cell kill in HNSCC.

Collectively, these data provide a strong rationale for pursuing additional studies of JNKs as potential therapeutic targets in HNSCC and possibly other malignancies. Other studies have suggested that JNKs can act as a tumor suppressor in fibroblast transformation (50). Hence, it will be important to gain a deeper understanding of the mechanistic basis for the different roles of JNKs in tumors if the full potential of JNK inhibitors as anticancer therapies is to be understood. As for many other treatments, inhibitors of JNKs may prove useful in the treatment of certain tumor types but not others. The development of compounds with greater selectivity for individual JNK isoforms than SP600125 will provide new insights into the role of JNK1, JNK2, and JNK3 in carcinogenesis. Because JNKs are relevant to cell biology in general, developing agents with an acceptable therapeutic index may also prove challenging until more selective agents are developed.

Acknowledgments

We thank Celgene Corporation for the generous support of providing SP600125, and Drs. Rama Narla and Steven Sakata for their expert advice on matters related to drug preparation and delivery.

References

1. Ip YT, Davis RJ. Signal transduction by the c-Jun N-terminal kinase (JNK)—from inflammation to development. Curr Opin Cell Biol 1998;10:205–19.
2. Karin M. The regulation of AP-1 activity by mitogen-activated protein kinases. J Biol Chem 1995;270:16483–6.
3. Martin JH, Mohit AA, Miller CA. Developmental expression in the mouse nervous system of the p493F12 SAP kinase. Brain Res Mol Brain Res 1996;35:47–57.
4. Davis RJ. Signal transduction by the JNK group of MAP kinases. Cell 2000;103:239–52.
5. Kayahara M, Wang X, Tournier C. Selective regulation of c-jun gene expression by mitogen-activated protein kinases via the 12-*o*-tetradecanoylphorbol-13-acetate-responsive element and myocyte enhancer factor 2 binding sites. Mol Cell Biol 2005;25:3784–92.
6. Dong Z, Birrer MJ, Watts RG, Matrisian LM, Colburn NH. Blocking of tumor promoter-induced AP-1 activity inhibits induced transformation in JB6 mouse epidermal cells. Proc Natl Acad Sci U S A 1994;91:609–13.
7. Young MR, Li JJ, Rincon M, et al. Transgenic mice demonstrate AP-1 (activator protein-1) transactivation is required for tumor promotion. Proc Natl Acad Sci U S A 1999;96:9827–32.
8. Adjei AA. Blocking oncogenic Ras signaling for cancer therapy. J Natl Cancer Inst 2001;93:1062–74.
9. McDonald JS, Jones H, Pavelic ZP, Pavelic LJ, Stambrook PJ, Gluckman JL. Immunohistochemical detection of the H-ras, K-ras, and N-ras oncogenes in squamous cell carcinoma of the head and neck. J Oral Pathol 1994;23:342–6.
10. Yang YM, Bost F, Charbono W, et al. C-Jun NH(2)-terminal kinase mediates proliferation and tumor growth of human prostate carcinoma. Clin Cancer Res 2003;9:391–401.
11. Ennis BW, Fultz KE, Smith KA, et al. Inhibition of tumor growth, angiogenesis, and tumor cell proliferation by a small molecule inhibitor of c-Jun N-terminal kinase. J Pharmacol Exp Ther 2005;313:325–32.
12. Khatlani TS, Wislez M, Sun M, et al. c-Jun N-terminal kinase is activated in non-small-cell lung cancer and promotes neoplastic transformation in human bronchial epithelial cells. Oncogene 2007;26:2658–66.
13. Sacks PG, Parnes SM, Gallick GE, et al. Establishment and characterization of two new squamous cell carcinoma cell lines derived from tumors of the head and neck. Cancer Res 1988;48:2858–66.

14. Sacks PG. Cell, tissue and organ culture as *in vitro* models to study the biology of squamous cell carcinomas of the head and neck. Cancer Metastasis Rev 1996;15:27–51.

15. Hoteiya T, Hayashi E, Satomura K, Kamata N, Nagayama M. Expression of E-cadherin in oral cancer cell lines and its relationship to invasiveness in SCID mice in vivo. J Oral Pathol Med 1999;28:107–11.

16. Liggett WH, Jr., Sewell DA, Rocco J, Ahrendt SA, Koch W, Sidransky D. p16 and p16 β are potent growth suppressors of head and neck squamous carcinoma cells *in vitro*. Cancer Res 1996;56:4119–23.

17. Zou CP, Clifford JL, Xu XC, et al. Modulation by retinoic acid (RA) of squamous cell differentiation, cellular RA-binding proteins, and nuclear RA receptors in human head and neck squamous cell carcinoma cell lines. Cancer Res 1994;54:5479–87.

18. Weksler BB, Subileau EA, Perriere N, et al. Blood-brain barrier-specific properties of a human adult brain endothelial cell line. FASEB J 2005;19:1872–4.

19. Lowry OH, Rosebrough NJ, Farr AL, Randall RJ. Protein measurement with the Folin phenol reagent. J Biol Chem 1951;193:265–75.

20. Fox WD, Higgins B, Maiese KM, et al. Antibody to vascular endothelial growth factor slows growth of an androgen-independent xenograft model of prostate cancer. Clin Cancer Res 2002;8:3226–31.

21. Hoos A, Nissan A, Stojadinovic A, et al. Tissue microarray molecular profiling of early, node-negative adenocarcinoma of the rectum: a comprehensive analysis. Clin Cancer Res 2002;8:3841–9.

22. Patel MI, Subbaramaiah K, Du B, et al. Celecoxib inhibits prostate cancer growth: evidence of a cyclooxygenase-2-independent mechanism. Clin Cancer Res 2005;11:1999–2007.

23. Laemmli UK. Cleavage of structural proteins during the assembly of the head of bacteriophage T4. Nature 1970;227:680–5.

24. Towbin H, Staehelin T, Gordon J. Electrophoretic transfer of proteins from polyacrylamide gels to nitrocellulose sheets: procedure and some applications. Proc Natl Acad Sci U S A 1979;76:4350–4.

25. Kuntzen C, Sonuc N, De Toni EN, et al. Inhibition of c-Jun-N-terminal-kinase sensitizes tumor cells to CD95-induced apoptosis and induces G_2/M cell cycle arrest. Cancer Res 2005;65:6780–8.

26. Kainuma K, Katsuno S, Hashimoto S, et al. Differences in the expression of genes between normal tissue and squamous cell carcinomas of head and neck using cancer-related gene cDNA microarray. Acta Otolaryngol 2006;126:967–74.

27. Charalambous C, Pen LB, Su YS, Milan J, Chen TC, Hofman FM. Interleukin-8 differentially regulates migration of tumor-associated and normal human brain endothelial cells. Cancer Res 2005;65:10347–54.

28. Li A, Dubey S, Varney ML, Dave BJ, Singh RK. IL-8 directly enhanced endothelial cell survival, proliferation, and matrix metalloproteinases production and regulated angiogenesis. J Immunol 2003;170:3369–76.

29. Zenz R, Scheuch H, Martin P, et al. c-Jun regulates eyelid closure and skin tumor development through EGFR signaling. Dev Cell 2003;4:879–89.

30. Zenz R, Wagner EF. Jun signalling in the epidermis: From developmental defects to psoriasis and skin tumors. Int J Biochem Cell Biol 2006;38:1043–9.

31. Baselga J, Arteaga CL. Critical update and emerging trends in epidermal growth factor receptor targeting in cancer. J Clin Oncol 2005;23:2445–59.

32. Bonner JA, Harari PM, Giralt J, et al. Radiotherapy plus cetuximab for squamous-cell carcinoma of the head and neck. N Engl J Med 2006;354:567–78.

33. Shepherd FA, Rodrigues PJ, Ciuleanu T, et al. Erlotinib in previously treated non-small-cell lung cancer. N Engl J Med 2005;353:123–32.

34. Du L, Lyle CS, Obey TB, et al. Inhibition of cell proliferation and cell cycle progression by specific inhibition of basal JNK activity: evidence that mitotic Bcl-2 phosphorylation is JNK-independent. J Biol Chem 2004;279:11957–66.

35. Pedram A, Razandi M, Levin ER. Extracellular signal-regulated protein kinase/Jun kinase cross-talk underlies vascular endothelial cell growth factor-induced endothelial cell proliferation. J Biol Chem 1998;273:26722–8.

36. Tokuda H, Hirade K, Wang X, Oiso Y, Kozawa O. Involvement of SAPK/JNK in basic fibroblast growth factor-induced vascular endothelial growth factor release in osteoblasts. J Endocrinol 2003;177:101–7.

37. Albanell J, Codony-Servat J, Rojo F, et al. Activated extracellular signal-regulated kinases: association with epidermal growth factor receptor/transforming growth factor α expression in head and neck squamous carcinoma and inhibition by anti-epidermal growth factor receptor treatments. Cancer Res 2001;61:6500–10.

38. Kalyankrishna S, Grandis JR. Epidermal growth factor receptor biology in head and neck cancer. J Clin Oncol 2006;24:2666–72.

39. Hoshino S, Yoshida M, Inoue K, et al. Cigarette smoke extract induces endothelial cell injury via JNK pathway. Biochem Biophys Res Commun 2005;329:58–63.

40. Lee CC, Chen SC, Tsai SC, et al. Hyperbaric oxygen induces VEGF expression through ERK, JNK and c-Jun/AP-1 activation in human umbilical vein endothelial cells. J Biomed Sci 2006;13:143–56.

41. Naruishi K, Nishimura F, Yamada-Naruishi H, Omori K, Yamaguchi M, Takashiba S. C-jun N-terminal kinase (JNK) inhibitor, SP600125, blocks interleukin (IL)-6-induced vascular endothelial growth factor (VEGF) production: cyclosporine A partially mimics this inhibitory effect. Transplantation 2003;76:1380–2.

42. Li LF, Ouyang B, Choukroun G, et al. Stretch-induced IL-8 depends on c-Jun NH2-terminal and nuclear factor-κB-inducing kinases. Am J Physiol Lung Cell Mol Physiol 2003;285:L464–75.

43. Bernhard EJ, McKenna WG, Muschel RJ. Radiosensitivity and the cell cycle. Cancer J Sci Am 1999;5:194–204.

44. Bulgin D, Podtcheko A, Takakura S, et al. Selective pharmacologic inhibition of c-Jun NH_2-terminal kinase radiosensitizes thyroid anaplastic cancer cell lines via induction of terminal growth arrest. Thyroid 2006;16:217–24.

45. Ambrosini G, Sambol EB, Carvajal D, Vassilev LT, Singer S, Schwartz GK. Mouse double minute antagonist Nutlin-3a enhances chemotherapy-induced apoptosis in cancer cells with mutant p53 by activating E2F1. Oncogene 2007;26:3473–81.

46. Schwartz GK, Shah MA. Targeting the cell cycle: a new approach to cancer therapy. J Clin Oncol 2005;23:9408–21.

47. Dent P, Yacoub A, Fisher PB, Hagan MP, Grant S. MAPK pathways in radiation responses. Oncogene 2003;22:5885–96.

48. Potapova O, Haghighi A, Bost F, et al. The Jun kinase/stress-activated protein kinase pathway functions to regulate DNA repair and inhibition of the pathway sensitizes tumor cells to cisplatin. J Biol Chem 1997;272:14041–4.

49. Potapova O, Basu S, Mercola D, Holbrook NJ. Protective role for c-Jun in the cellular response to DNA damage. J Biol Chem 2001;276:28546–53.

50. Kennedy NJ, Sluss HK, Jones SN, Bar-Sagi D, Flavell RA, Davis RJ. Suppression of Ras-stimulated transformation by the JNK signal transduction pathway. Genes Dev 2003;17:629–37.